J Solid State Electrochem (2010) 14:2039–2048
DOI 10.1007/s10008-009-0985-0

ORIGINAL PAPER

Electropolymerization of pyrrole in acetonitrile as affected by the nature of substitute and deposition potential

Magdalena Graczyk-Zajac · Sergey Yu. Vassiliev · Mikhail A. Vorotyntsev · Galina A. Tsirlina

Received: 21 September 2009 / Revised: 22 November 2009 / Accepted: 26 November 2009 / Published online: 18 December 2009

Abstract We apply chronoamperometry and cyclic voltammetry to trace the effect of the deposition potential on morphological and redox properties of N-substituted polypyrrole films on platinum and ITO in acetonitrile solutions. The goal of these experiments is to check whether certain principle trends observed in the course of the film growth can be used to monitor the deposition process and to control the features of the fabricated polymer. We use STM for morphology characterization, and estimate the film thickness from its redox response in background solution. For titanocene-substituted pyrrole, we compare current transients data on the anodic electropolymerization and the monomer reduction, in order to estimate the mass transport contribution to the polymerization current within various time domains (0.1 ms–1,000 s). On the basis of all these observations, we conclude on the existence of four characteristic regions of deposition current transients and assign them to certain steps in the oligomers formation and the film growth. The region of the current growth is discussed as well in terms of traditional nucleation models.

S. Yu. Vassiliev (✉) · M. A. Vorotyntsev · G. A. Tsirlina
Department of Electrochemistry, Faculty of Chemistry,
Moscow State University,
119991 Moscow, Russia
e-mail: wasq@elch.chem.msu.ru

M. Graczyk-Zajac · M. A. Vorotyntsev
ICMUB-UMR 5260 CNRS, University of Burgundy,
21000 Dijon, France

Present Address:
M. Graczyk-Zajac
Darmstadt University of Technology,
Petersentr. 23,
64287 Darmstadt, Germany

Keywords Electropolymerization · Substituted polypyrrole · Nucleation · STM

Introduction

The morphology of conducting polymers is a feature important for numerous applications and usually essential for the redox behavior. At this stage, only occasional observations of the effect of the deposition mode on the film morphology are available. We consider below some trends, which are of interest for the future in the context of the controllable formation of films with a certain morphology. This problem is closely related to approaches allowing control and to monitor the total film thickness on the basis of the deposition current and charge transients. It looks attractive to apply these instruments, very informative for metal deposition, to a more complex process of the polymer growth.

Model approaches to the current transient analysis worked out for deposition of inorganic solids cannot be applied straightforwardly to the polymers deposition. Actually, in contrast to the metal electrocrystallization, deposition of conducting polymers is complicated by the preceding and parallel formation of soluble oligomers, and the current efficiencies are frequently not too high. Current transients typical for the polymer deposition start from the region of current decrease, with a subsequent minimum [1–11]. This initial region is formally treated as induction period. No formation of a solid product in this time domain (before the onset of the current increase) was found by ellipsometry for pyrrole [3] and thiophene [6] polymerization; the evident changes of optical interfacial properties were observed only after passing the minimum, i.e., at the ascending branch of the current transient. However, this

does not mean automatically that this branch can be analyzed as a deposition transient without any correction for the oligomer formation.

We try to understand the nature of monomer oxidation processes in various time domains and to interrelate the observed morphological features and the transient shape for pyrrole monomers with essentially different substitutes. Our special attention to effects of the monomer substitute originates from the molecular nature of film fragments (chains forming perfectly shaped particles) and an important role of spatial factors in geometry of these fragments. For relatively thin films of conducting polymers, the most usual morphology is a set of overlapped 3D fragments having a more or less symmetric (spherical-like) shape. We do not discuss here any dendritic or other complex morphological types of electrodeposited polymer films, as these morphologies correspond mostly to thicker deposits. Our experiments are limited to 100–200-nm thick films (or even thinner), because for thicker electrodeposited polymers one can hardly avoid an essential cross-section inhomogeneity.

Experimental

Electroactive polymer denoted as pTc3Py possesses a polypyrrole matrix, with titanocene dichloride centers (Cp_2TiCl_2, Tc) attached to the matrix via aliphatic (propyl) chains. Solid monomer $C_4H_4N(CH_2)_3C_5H_4(TiCl_2)C_5H_5$ (Tc3Py) was synthesized as described in Ref. [12]. Poly (*N*-methyl-pyrrole) was studied in parallel experiments. *N*-methyl-pyrrole was freshly distilled and kept under Ar. Polymers were deposited from 0.1 M $TBAPF_6$ acetonitrile solution (estimated water content in solution was of the order of 500 ppm, water was introduced by both the solvent and supporting electrolyte, see Ref. [12, 13] for further details).[1] We do not return to the effect of the supporting anion nature and the concentration discussed in [9, 14]. Monomer concentration was always 1 mM, in order to extend the timescale of any nucleation and/or growth events and to have a better chance to compare the polymerization of monomers with different oxidation rates/oligomer solubilities.

Films of 50–150-nm thickness (see the methods of in situ thickness estimation in Refs. [12, 16]) were deposited under potentiostatic mode on Pt and ITO supports with the surface areas of 0.01 and about 0.5 cm^2, respectively. The majority of electrochemical experiments are related to polymer films on polycrystalline Pt disc.

All electrochemical experiments were performed after removal of oxygen from solution by the vacuum pumping procedure, followed by filling the cell with argon, then the solution was kept under argon atmosphere in a conventional single-compartment cell with platinum wire counter electrode and Ag/(0.01 M $AgNO_3$+$TBAPF_6$ in CH_3CN) double junction reference electrode. All potentials below are referred to this reference electrode (its potential, including diffusion potential drop, is about 0.33 V versus aqueous SCE). Autolab PGSTAT30 potentiostat (Ecochimie, The Netherlands) equipped with ADC750 module provided 1.5-μs time resolution. Other details can be found in Refs. [12, 13, 17].

All STM measurements were performed using the commercial *ex situ* scanning tunneling microscopes LitScan and "UMKA" (Concern "Nanoindustry", Moscow), both equipped with extended spectroscopic facilities. Pt-Ir tip (10% Ir) of 0.5 mm diameter was mechanically sharpened. For topographic measurements, −0.3 V tunneling voltage was applied (positive voltage corresponds to positive sample polarization), in combination with 0.3–0.8 nA tunneling current (the exact value was specially chosen for each type of sample). The samples were washed with acetonitrile (to remove the soluble oligomer phase and salts from the surface) and dried in air at temperatures up to 50 °C.

The technique of local tunneling spectroscopy at certain fixed points was described in detail in Ref. [18]. The height-voltage spectroscopy was used to estimate of tip-sample distance and to detect the oligomeric phase. Pronounced changes in tip height (or step-like behavior of spectra when ramping the tip voltage with feedback switched on) manifest the presence of low-conducting and/or redox-active layer on the surface of the polymer deposit [18].

Results and discussion

Characterization of films formed at different potentials

A general feature of all potentiostatic deposition transients is a noticeable induction period with no formation of any rechargeable film. The duration of this period appeared to be dependent on the nature of substitute in the monomer molecule.

Potentiostatic deposition from *N*-methyl-pyrrole solution typically demonstrates a very low current during the induction period and a sharp current increase, with a clear

[1] It was recognized long time ago that even a low water content in acetonitrile affects catastrophically the polythiophene polymerization [5, 6], but improves the quality of polypyrrole films [4, 5, 15]. We should mention that our water content is far below the concentration recommended in [5] (0.1 M H_2O) for pyrrole, since the latter can affect the state of chemically active Tc substitutes, up to their hydrolysis.

nucleation maximum (Fig. 1). The STM visualization (Fig. 2) of films having approximately equal thicknesses (controlled by the deposition charge) indicates a relatively wide size distribution of small particles (8–15 nm in radius) forming a more or less smooth layer. The flatness of the polymer film disrupts with increase of the deposition potential. For large geometric area electrodes, microstructure details differ markedly along the sample surface, indicating rather different deposition conditions in various points. We can assume that this lateral inhomogeneity results from an inhomogeneous potential distribution along the large surface in the weakly conducting solution, or from a less regular contribution of diffusion or convection fluxes in solution. Local tunneling spectroscopy demonstrates the presence of a thick oligomeric (less conductive) layer outside the deposited polymer. However, the conductivity of this external layer (insoluble in acetonitrile) is enough to stabilize the STM feedback at a low current.

Potentiostatic current transients obtained for Tc3Py demonstrate a shorter induction period, but a more substantial charge passed in this region. At potentials below 0.7 V, no film formation was observed by means of both microscopy and voltammetry in background electrolyte. The current minimum is observed in the whole potential range, and the current increases slower as compared to *N*-methyl-pyrrole at the same potential. Within a more extended time range, oscillations can be noticed in some transients (Fig. 3).

Samples of pTc3Py not subjected to cleaning (by washing with acetonitrile) cannot be visualized using STM, because of a large amount of poorly conducting viscous (liquid-like) fragments. We attribute this easily soluble component to oligomers with relatively short chain lengths. In thicker films, two types of fragments with different conductivities (as judged from local tunneling spectra) were discovered even after cleaning. We assume that the molecular weight of codepositing oligomers increases in the course of the prolonged deposition, and it is more difficult to dissolve the oligomeric component from thick films (these oligomers can be also treated as less crystalline amorphous polymer of a lower molecular weight). If the chemical nature of oligomers and polymers is identical, and there are no specific terminal groups, the conductivity is mostly affected by crystallinity and conjugation degree (correlating in its turn with the chain length) [19], i.e., it increases with the chain length. This is why we assign the fragments of lower and higher conductivities to less crystalline oligomers and polymers, respectively. In pTc3Py, the content of less conducting phase increases with the film thickness.

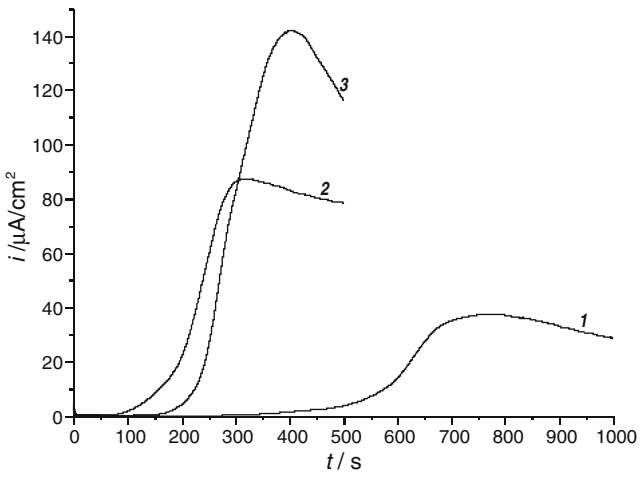

Fig. 1 Potentiostatic deposition transients of poly(*N*-methyl-pyrrole) on ITO at 0.67 (*1*), 0.69 (*2*) and 0.71 V (*3*)

The morphology of cleaned deposits is characterized by a narrow size distribution of polymer particles (ca. 12 nm radius, Fig. 4). It is very close to the mean radius for poly(*N*-methyl-pyrrole) (ca. 11 nm). Sphere-like shape of separate polymer particles observed for both pTc3Py and poly(N-methyl-pyrrole) manifests the 3D growth of the nuclei of principle phases. A tendency to form large flat 2D-clusters of aggregated particles (2D layer-by-layer growth of the ensemble of 3D-particles) is clearly seen at low and medium overvoltages. Less regular mountain-like structure is formed at high overvoltages. Note that all pTc3Py samples under study were of approximately equal thicknesses controlled by the deposition charge (Fig. 3), this is why the observed disordering at higher potentials cannot be assigned to the difference in support contribution and/or of growth inhomogeneity normal to the surface. In contrast to poly(*N*-methyl-pyrrole), tunneling spectroscopic measurements fail to detect any essential amount of the low-conducting oligomeric phase on the top of thin (up to 100 nm) polymer films after preliminary cleaning in acetonitrile. The conductivity of the crystalline pTc3Py seems to be somewhat lower than that of poly(*N*-methyl-pyrrole).

For both substituted monomers, we performed the deposition in a wide potential interval, and checked the effect of deposition potential on the redox behavior of the film. The current efficiency of the polymer formation varies in the range of 70–90% [17] and depends on both deposition time and deposition potential. Correspondingly, the accuracy of our coulometric control in the course of the deposition can be insufficient for fabrication of a series of films with an exactly constant thickness.

To make our comparison of films of different thicknesses more informative, we applied the normalization procedure for redox properties of films in background solution (charge, current) with respect to the deposition charge, Q_{dep}. The basis of this approach is an approximately linear dependence of the anodic and the cathodic redox charges,

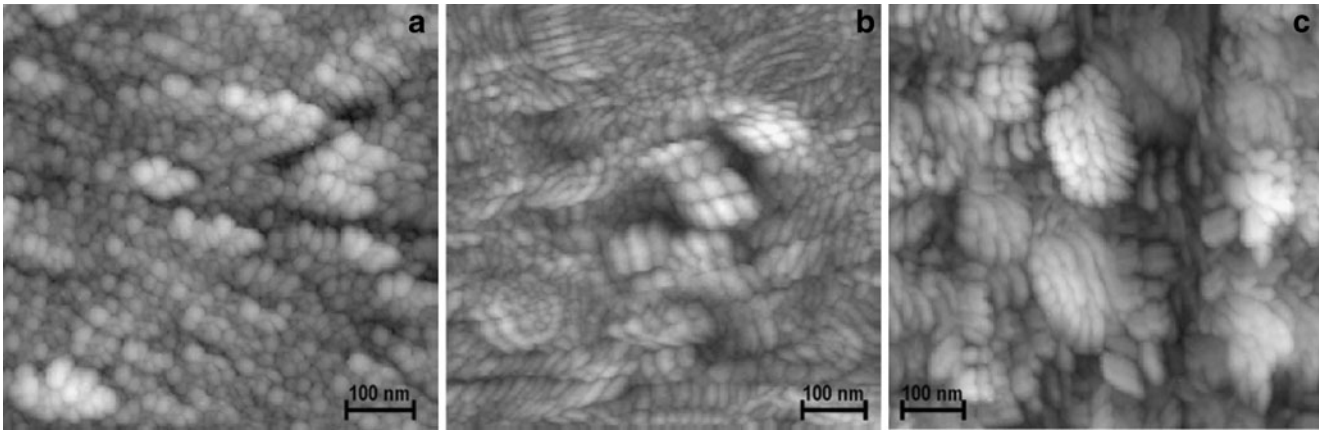

Fig. 2 STM-images of poly(*N*-methyl-pyrrole) on ITO deposited at 0.67 (**a**), 0.69 (**b**), and 0.71 V (**c**) under potentiostatic conditions (see Fig. 1 for deposition transients)

Q_+ and Q_- (measured in monomer-free solution), on Q_{dep} at a constant deposition potential (Fig. 5). The slope of such a plot can be used to estimate the deposition efficiency [17, 20]. We also compared the data for a series of films fabricated with the same deposition charge in a freshly prepared solution and after several depositions from this solution. The reproducibility can be judged from two couples of points at Q_{dep}=125 μC in Fig. 5, it is comparable with the accuracy of the Q_+ and Q_- calculation. Q_+ is usually a bit higher than Q_-. In what follows, Q_+ was used for efficiency calculations.

The zero intercept of the line in Fig. 5 should also be considered as approximation, because of a pronounced scattering of experimental points. The existence of this linear correlation allows us to compare voltammetric responses of films corresponding to different deposition charges, Q_{dep}, by dividing the redox current by the charge, I/Q_{dep}, in order to see the variation of the deposition efficiency and of the shape of the redox response for a series of deposition potentials. To retain the current as the dimension of such "normalized responses", we multiply all values of the above ratio by a "standard deposition charge", Q_{dep}^0=125 μC, so that $I_{norm}=I_{exp}\ Q_{dep}^0/Q_{dep}$.

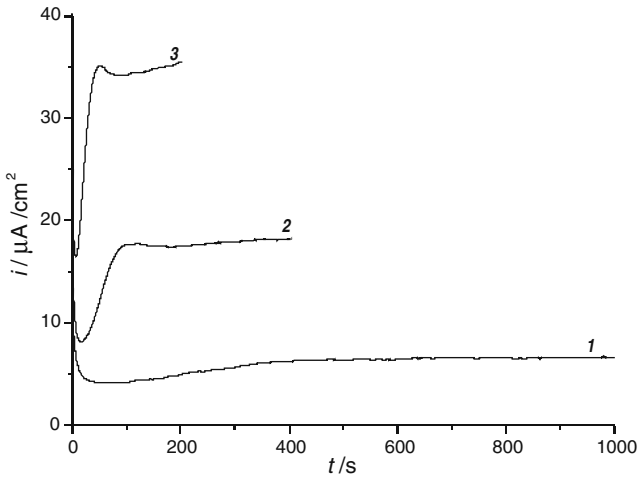

Fig. 3 Potentiostatic deposition transients for pyrrole modified by Tc centers (Tc3Py) on ITO at 0.7 (*1*), 0.75 (*2*), and 0.8 V (*3*). The shape of transients at 0.7 V is reproducible, but current values are very sensitive to temperature

Figure 6 presents such normalized voltammograms, I_{norm}, of pTc3Py films deposited at various potentials. It is easy to see that the potential range corresponding to the highest deposition efficiencies is rather narrow. At lower potentials, the efficiency is low because of preferential oligomer formation. As for higher potentials, it is well known that the oxidative degradation in this potential range starts already in the course of deposition [1, 2, 4, 14]. A similar tendency has been observed for *N*-methyl-pyrrole deposited at various potentials (Fig. 7). The efficiency losses have been, in that case, less significant.

To summarize, both substituted pyrroles demonstrate "polymer-oligomer codeposition" (more precisely, codeposition of substances of different conductivities). For Tc3Py, the fraction of less crystalline oligomeric codeposit is much higher, or its conductivity is much lower. In all cases the STM-visualization is possible only after partial dissolution of a gel-like component. Qualitatively, the nature of the pyrrole substitute (its geometrical dimensions or chemical composition) can markedly change the kinetics of electrochemical and chemical processes accompanying the polymerization, as well as the final microstructure of the deposited polymer. For two substituted pyrrole films under comparison, we clearly observe an effect of the attached functional group on the potential-morphology interrelation. In both cases, the faster is the deposition, the stronger is a morphological non-uniformity. However, particular details are different: for *N*-methyl-pyrrole, the increase of the potential results in formation of more shaped globulas

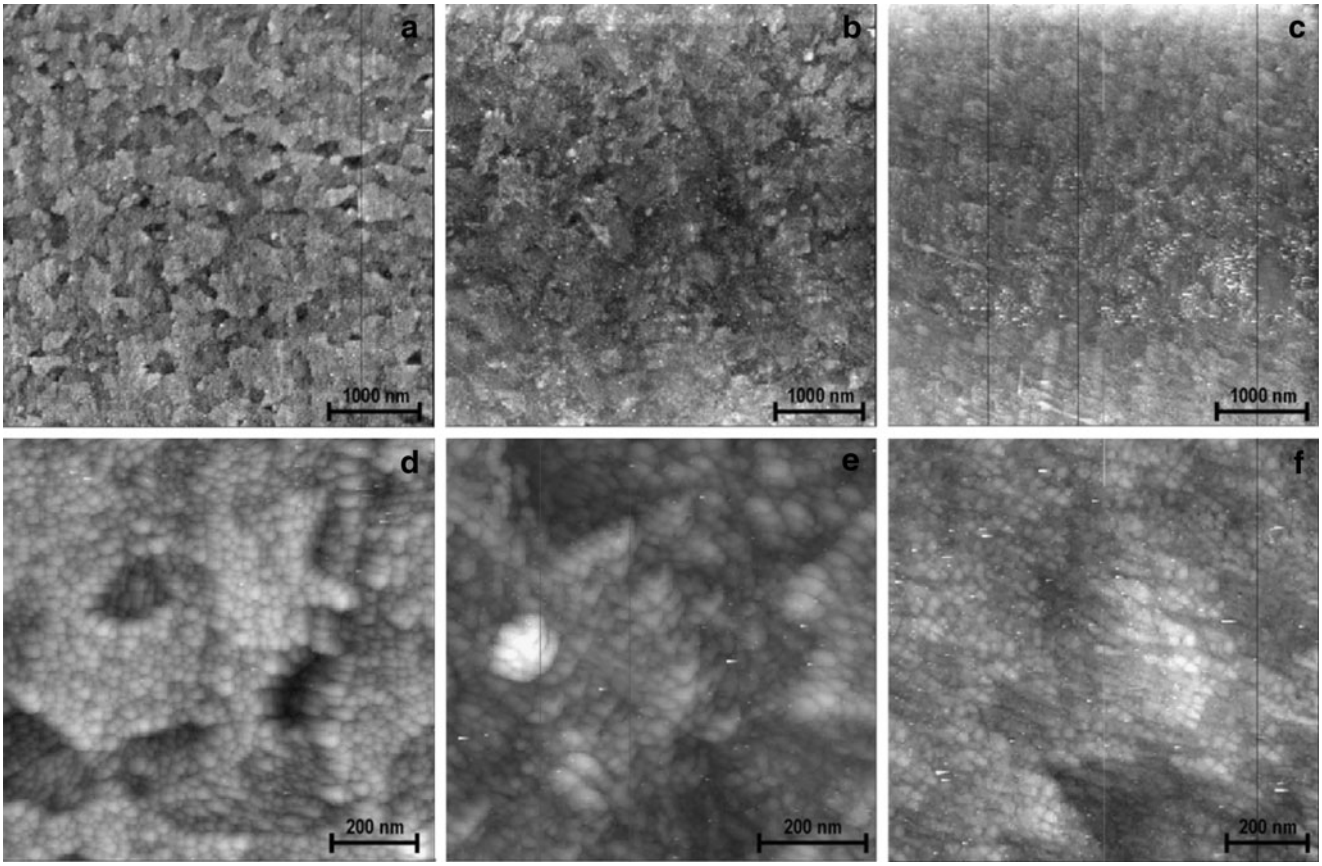

Fig. 4 STM-images of polypyrrole modified by Tc centers on ITO deposited at 0.7 (**a**, **d**), 0.75 (**b**, **e**), and 0.80 V (**c**, **f**) under potentiostatic conditions (see Fig. 3 for deposition transients)

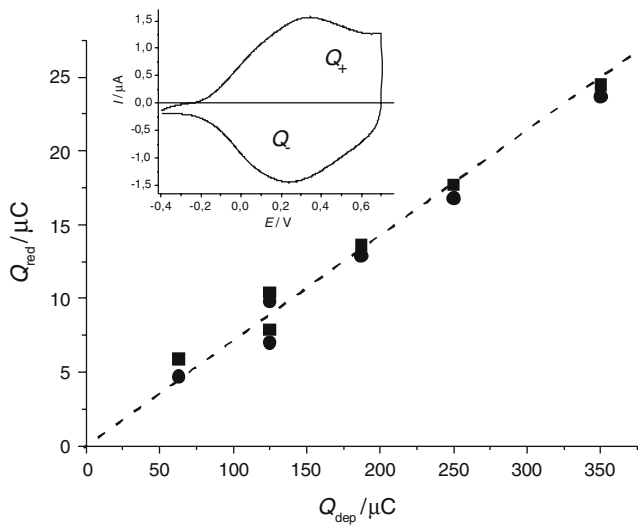

Fig. 5 Redox charge of p film as a function of the polymerization charge (*squares* represent Q_+ and *circles*, Q_-). Deposition potential E= 0.8 V, sequence of depositions charges: 125, 63, 187, 250, 350, and 125 µC (lower efficiency). Geometric electrode area is 0.01 cm^2

(consisting of invariable nanometer-size fragments), whereas for pTc3Py we observe a pronounced decrease of the size of these fragments without appearance of any evident globular substructure.

General transient behavior

Nucleation-growth phenomena for pyrrole polymerization were first addressed by the Pletcher's group [1] in the study of aqueous monomer solutions at various pH.

Diffusion controlled growth was assumed earlier for poly(*N*-methyl-pyrrole) [2], in contrast to non-substituted pyrrole polymerizing under the electron transfer control. These conclusions were made on the basis of an indirect evidence (model treatment of current transients), and the reasoning remained questionable, as well as a mechanism of the electrode reaction responsible for nucleation. Formal kinetic analysis given in Ref. [21] demonstrated the reaction order to be equal to unity with respect to the monomer concentration. The adsorption of monomer was assumed to be the initial step, but this conclusion cannot be extended automatically to non-aqueous media and/or to substituted monomers. According to the analysis of

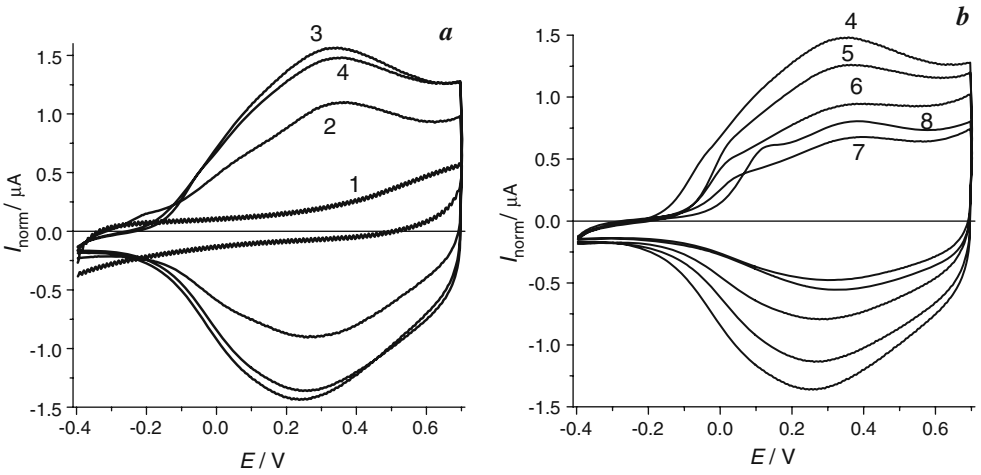

Fig. 6 Normalized redox responses of pTc3Py films deposited at different potentials (*in brackets* the ratio of the redox charge to the deposition charge, $Q_{red}/Q_{dep} \cdot 100\%$): **a** 0.7 V (no film formation, curve 1), 0.75 V (5.7%, curve 2,), and 0.8 V (8%, curve 3) and **b** 0.85 V (7.7%, curve 4), 0.9 V (6.2%, curve 5), 0.95 V (4.8%, curve 6), 1 V (3.4%, curve 7), and 1.05 V (3.8%, curve 8). See text for the normalization procedure. Geometric electrode area is 0.01 cm^2

voltammetric data and current transients for pyrrole polymerization in aqueous medium [11], the limiting step is the first single electron transfer.

The main problem of nucleation models application (even formal) is to attribute the current (charge) to the new phase formation. This problem looks less crucial for *N*-methyl-pyrrole, as the analysis of *I*,*t*-dependence can be simply started from a certain moment, $t>0$, taken as the onset of the nucleation process.

Another problem is to apply nucleation-growth models to transient regions corresponding exclusively to primary nucleation. The globular morphology presented in Figs. 2 and 4 agrees with assumption that in the course of polymer deposition the growth of the primary nuclei stops, and new nucleation event takes place on the surface of the polymer particle. Correspondingly, polymer growth consists in continuous nucleation events. Below this behavior is discussed as "secondary nucleation". It is well known, for example, for electrodeposition of highly dispersed platinum group metals from chloride bath [22, 23], under conditions of pronounced self-inhibition of the primary growth. This phenomenon was discussed for deposition of polymers as well [24]. For polymers it can results from the rupture of growth at a certain length of the polymer chain (death-and-rebirth mechanism). Search for "death" reason is surely out of the scope of this study, but we can assume that it is of a chemical nature (chain rupture is typical for many polymerization processes). To estimate the time when the secondary nucleation starts, one should calculate the charge necessary for formation of a single layer of particles with sizes found from microscopy, and then to correlate it with time intervals at experimental transients. For majority of transients registered for the two systems under discussion this characteristic time corresponds to the end of the

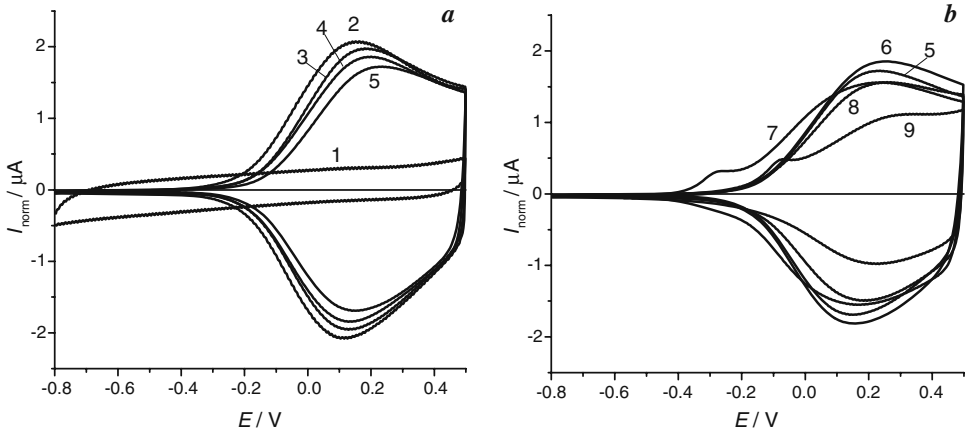

Fig. 7 Normalized redox responses of poly(*N*-methyl-pyrrole) films deposited at different potentials (*in brackets* the ratio of the redox charge to the deposition charge, $Q_{red}/Q_{dep} \cdot 100\%$): **a** 0.6 V (no film formation, curve 1), 0.65 V (8,4%, curve 2,), 0.68 V (7,8%, curve 3), 0.72 V (7,3%, curve 4,), and 0.78 V (6,7%, curve 5) and **b** 0.78 V (6.7%, curve 5), 0.82 V (6.5%, curve 6), 0.85 V (7%, curve 7), 0.9 V (6.1%, curve 78), and 1 V (4,4%, curve 9). See text for the normalization procedure. Geometric electrode area is 0.01 cm^2

ascending branch or to the beginning of the plateau, see the discussion below.

For the less studied Tc-substituted monomer, we attempted to approach the solution of these problems by providing a deeper analysis of the dependence of the transient shape on the potential for different time domains (Fig. 8a). Major trends are qualitatively the same as reported earlier for various polymers [1, 2, 4, 5, 7, 11]: starting from certain threshold potential, the monotonous decay changes for the curve with a current minimum; the latter is shifted towards a shorter time when the potential increases, and simultaneously the time when the plateau starts becomes shorter; finally, the plateau current increases. The appearance of a broad and weak current maximum at the beginning of the plateau was observed from time to time at relatively high potentials, but this feature was less reproducible.

The specific regions of transients are considered subsequently below.

The region of current decrease (Fig. 8b) does not demonstrate a Cottrell-like behavior mentioned earlier for other electropolymerization processes [3, 7]. These deposition data are also compared in Fig. 8b with the current transient of a purely diffusional process, electroreduction of the same Tc3Py monomer at a sufficiently high overvoltage (dashed line in Fig. 8b), i.e., a system with exactly the same mass transport parameters.

According to treatment of ellipsometric data [3], the formation of a single monolayer of the depositing substance can be assumed in the region of current decrease. In the earlier ellipsometric study [10], it was concluded that in this region oligomers are already attached to some special (rarely distributed) very active centers. From comparison of the data for potential steps in supporting and monomer-containing solutions, one can deduce that the monomer oxidation starts at potentials at least 0.2–0.3 V more negative than the typical potential of nucleation manifestations (at least if we consider time periods within 10^3 s order).

The next characteristic region ("bottom", and probably the initial portion of the rising branch) already corresponds to formation of very thin rechargeable films (Figs. 6 and 9). A similar experiment was earlier described in [6] for polythiophene in dry acetonitrile. When the anodic polarization was interrupted in the point of the current minimum, no evidence of the film formation was found, while if the same change-over to a lower potential was made in the region of the current plateau, the cathodic current appeared because of the discharge of an already formed film. In [10] it was assumed that in this region the nucleation starts at a major portion of the surface, and the polymer is formed in between of initially attached rare oligomers. We should mention that this hypothesis cannot explain the observed increase of the current.

The region of current increase corresponds expectedly to the solid product formation. Figure 9 demonstrates our coulometric estimates of the film thickness (see Ref. [17]) for the points of the minimum and of the current stabilization (see arrows in Fig. 8 above). In the former case this formal estimate gives 2.5–5 nm, and there is no evident potential effect. These values correspond to several molecular monolayers, but it is evident that some portion of the charge before minimum corresponds to the formation of soluble products, and there is no indication of the formation of any 3D solid product. As for the *current stabilization*, it starts at effective thicknesses of 20–30 nm (being higher for lower potentials). A monolayer of polymer particles of 10–13 nm in radius is expected to be formed just in the vicinity of the current stabilization. The uncertainty still exists with some very thin underlayers, which cannot be directly visualized, but its contribution to the deposition charge is comparable with the accuracy of our particle size estimates.

For *N*-methyl-pyrrole (Fig. 10), different characteristic time intervals of the abovementioned regions are observed, but all general trends remain the same.

Note, that in Ref. [3] the formation of a 'primary polypyrrole layer' (underlayer, with a thickness of a few nm) was assumed, with a parallel formation of 3D film. The film density was found to be thickness-dependent for the thicknesses up to 30 nm. The same feature was noticed for a bottom layer of the polythiophene film [6] and assumed for polypyrrole [10]. For polyaniline, ellipsometric/EQCM data led to the conclusion about a denser bottom layer, with the growth of a subsequent less dense layer starting in the region of the current increase [25]. The same conclusion about the initial formation of a non-porous layer was mentioned for polythiophene [26].

Formal analysis of kinetics at early deposition steps

As the ascending branch of the transients (excluding its upper part) corresponds to the formation of the first layer of polymer "nuclei",[2] we apply the traditional nucleation-growth approach, i.e., consider d log I/d log t values. Our I vs t^n dependences correspond approximately to n=2, in agreement with the earlier data for non-substituted and *N*-

[2] For highly irreversible polymerization, the notion of nucleation in its classical meaning for reversible processes cannot be used as exact term. In what follows we apply "nuclea" and"nucleation" in purely geometric sense, i.e., for appearance of some fragments of growing polymer. Note that very restricted versions of nucleation models discussed in this paper deal with the nuclea only in geometrical sense.

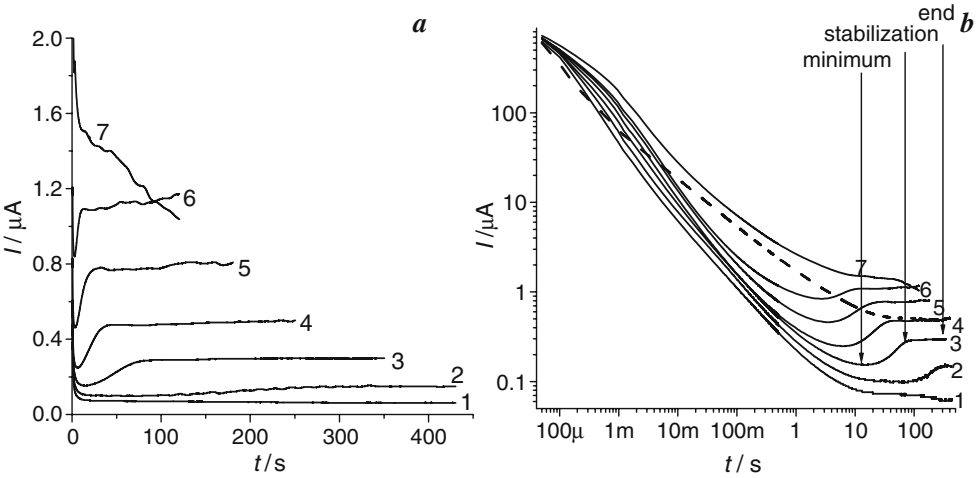

Fig. 8 Current transient of the pTc3Py potentiostatic deposition on platinum at different potentials: 0.6 V (*1*), 0.75 V (*2*), 0.8 V (*3*), 0.85 V (*4*), 0.9 V (*5*), 0.95 V (*6*), and 1.1 V (*7*) in usual (**a**) and bi-logarithmic (**b**) coordinates; *dashed line* (plot b) presents a current-time transient of the titanocene dichloride reduction. *Arrows* indicate characteristic integration limits (for curve 3, to give an example) used to calculate Q_{min}, Q_{stab}, and Q_{dep}. Geometric electrode area is 0.01 cm^2

methyl substituted pyrroles [1, 2, 5], as well as for polyaniline if the monomer concentration was high [8].

For a further correct application of this approach we should limit ourselves to a certain time domain in which the nature of the electrochemical reaction remains unchanged. According to [27], the number of electrons transferred to one reacting monomer species in the course of its oxidation is time dependent, increasing from 1 within the short time domain to ca. 2.5 at a longer time scale. For all potentials considered below the ascending branch corresponds to the predominating kinetic control and a constant number of transferred electrons [27].

It is not so easy to distinguish between the models leading to the same power, n, in $I=const \bullet t^n$ dependence. Basically, $n=2$ corresponds to the kinetic control (instantaneous 3D nucleation or progressive 2D nucleation). Of course, we can consider the results for the I vs t^n dependence as reliable only in combination with other experimental manifestations corresponding to the same nucleation model. The simplest additional test is the dependence of the slope of I, t^n -curves on the electrode potential, E, since a specific behavior for dI/dt^n vs E is predicted for each model. An analysis of this sort is reported in Refs [1, 2, 8] for instantaneous 3D nucleation. The resulting dependences are in a good agreement with independently obtained kinetic data, and demonstrate no contradictions with the predictions based on the model assumed from n value. In [28], a similar treatment is proposed for "mixed" (simultaneous 2D and 3D) nucleation.

For the films under study, 3D versions look more justified, as can be judged from the images in Figs. 2 and 4. For 3D instantaneous nucleation and growth of semi-spherical nuclei under the kinetic control, the current of the ascending branch of the transients can be expressed as [29]:

$$I(t) = N \bullet \frac{2\pi V_M^2 i_0^3}{z^2F^2}\left\{\exp\left(\frac{\alpha zF\eta}{RT}\right) - \exp\left(-\frac{(1-\alpha)zF\eta}{RT}\right)\right\}^3 t^2,$$

N is the number of active centers per unit area, i_0 is the exchange current density, V_M is the molar volume of polymer, z is the number of electrons transferred per monomer species, α is the transfer coefficient, and η is the overvoltage. At a high overvoltage, one can neglect the second exponent:

$$\log\left(\frac{dI(t)}{dt^2}\right) = \log\left(N \bullet \frac{2\pi V_M^2 i_0^3}{z^2F^2}\right) + 3 \bullet \frac{\alpha zF}{2.3RT} \bullet \eta$$

Specific features of the polymer deposition (induction period at $t< t_0$, pronounced contribution of soluble product formation and background processes I_0) complicate strongly the data analysis. For a more correct treatment, the observed current should be considered as $I(t)=I_0+k(t-t_0)^2$. This functional form does not allow of identifying in bi-logarithmic coordinates the interval which corresponds to the parabolic behavior of the partial current of the polymer deposition. In addition, the uncertainty of the I_0 and t_0

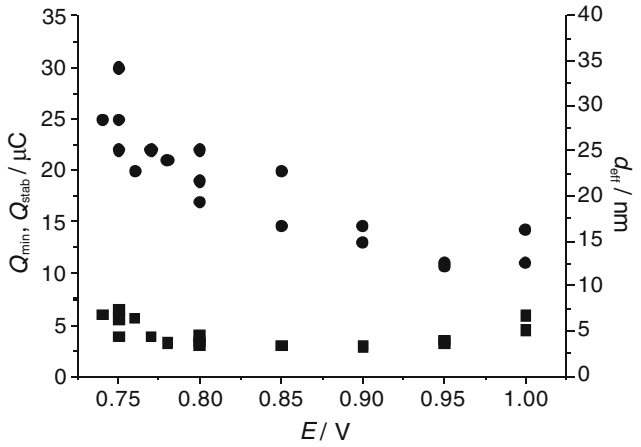

Fig. 9 Deposition charge and effective thickness corresponding to the minimum (*solid boxes*) and current stabilization (*solid circles*) of the transient. Geometric electrode area is 0.01 cm^2

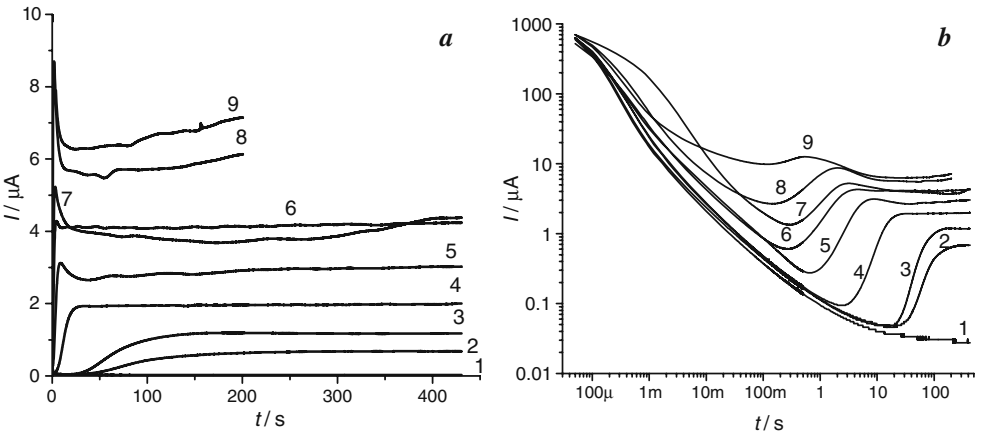

Fig. 10 Current transient of poly(*N*-methyl-pyrrole) potentiostatic deposition on platinum at different potentials: 0.6 V (*1*), 0.65 V (*2*), 0.68 V (*3*), 0.72 V (*4*), 0.78 V (*5*), 0.82 V (*6*), 0.85 V (*7*), 0.9 V (*8*), and 1 V (*9*) in usual (**a**) and bi-logarithmic (**b**) coordinates. Geometric electrode area is 0.01 cm^2

values makes the results ambiguous, so that all these parameters have to be determined from the fitting procedure. There are no technical details on the dI/dt^2 calculation in Refs. [1, 2, 8], so we cannot estimate whether the applied procedures took into account the above mentioned problem. In what follows we assume that for rather short period of the primary nucleation, I_0 is approximately constant, and $dI(t)/dt = 2k(t-t_0)$. Under this assumption one can obtain the slope k from a linear approximation of $dI(t)/dt$ vs. t dependence. It is easy to do a visual separation of the linear portion of this dependence. We found that *ca.* one third of the ascending branch of the transients follows the parabolic law. For Pt support, this region corresponds to 1–20 s for Tc3Py and 0.1–20 s for *N*-methyl-pyrrole (exact values depend on the overvoltage).

Our dI/dt^2 potential dependences are compared with the same data extracted from [1, 2] (Fig. 11). At low overvoltages resulting in films with a high redox activity (0.65–0.75 V for *N*-methyl-pyrrole and 0.75–0.8 V for Tc3Py), we found a linear dI/dt^2 vs E dependence. The slopes for acetonitrile solutions (curves 3–8 in Fig. 11) are slightly lower as compared to those for aqueous medium [1, 2] (curves 1, 2 in Fig. 11). At higher overvoltages, where a high redox activity is partly lost because of the oxidative degradation, a systematic deviation from linearity can be noticed. We assign it to the increase of ohmic losses, hardly avoidable in nonaqueous solutions, or to changes of kinetic parameters due to the contribution of a deeper oxidation. Basically, all the slopes are rather close, evidencing similar kinetic peculiarities for all systems under comparison.

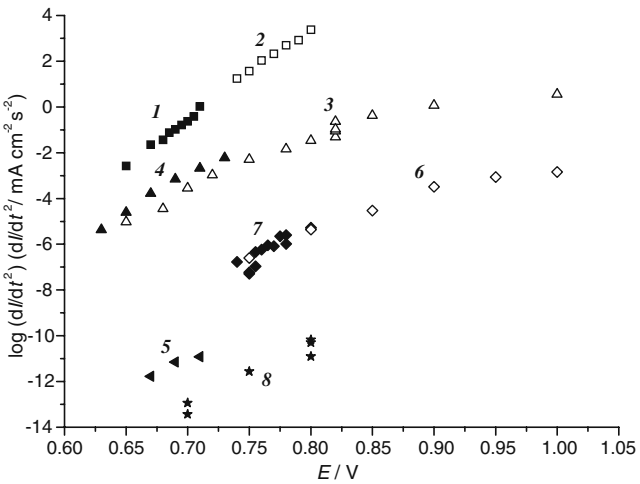

Fig. 11 Plots of the slopes of I vs. t^2 taken from Fig. 8 in [1] (pyrrole, aqueous solution) (*1*), from Fig. 3 in Ref. [2] (*N*-methyl-pyrrole, aqueous solution) (*2*) and from our transients for poly(*N*-methyl-pyrrole) (*3–5*); and pTc3Py (*6–8*) deposition in acetonitrile solution on Pt (*3*, *4*, *6*, and *7*) and ITO (*5*, *8*). To compare the data, we use the same potential axis, but potential values in Ref. [1, 2] correspond to aqueous SCE

Intercepts for aqueous and acetonitrile solutions cannot be compared because of potential scales incompatibility. However, comparison of these values for Pt and ITO supports in acetonitrile probably indicates a much lower value of N for ITO. A higher number of active centers on metals as compared to those on oxides is typical for various electrodeposition processes. Another reason can be a lower exchange current density for the controlling electrochemical step. As the monomer oxidation starts directly at the surface of the support, electrocatalytic properties of the latter can play an important role in initial deposition steps (at not too-long deposition time).[3] An essential difference of the nucleation kinetics for various supports is reported in Ref. [11] and discussed just in terms of the different electrocatalytic activity. The explanation based on the effect of support on the reaction pathway and the nature of the limiting step (which can be considered as a specific sort of electrocatalysis) is hardly possible, as the formal kinetic parameter, αz , discussed below remains the same. This parameter is roughly specific for a certain reaction step.

[3] The abovementioned analysis was done for initial stages of primary nucleation, when the electrochemical reactions take place mainly at the support surface. The formation of dense monolayer of polymer particles is expected only in the region of current stabilization (Fig. 9). For long-time domain, the kinetics of monomer oxidation is surely determined by polymer properties, not by any electrocatalytic effects of the support surface.

An formal estimate of αz results in rather reasonable values, 0.4–0.7, being higher for N–methyl-pyrrole. Formal parameter, αz, if being obtained for a multistep reaction, depends on the transfer coefficient of the limiting step, α_s, the number of its repetitions, v, and the number of preceding fast steps, z_f, according to equation $\frac{z_f}{v} + \alpha_s$, [30]. However, both the values reported in Ref. [11] and obtained in this study favor the slowness of the first step (z_f=0), so most probably α_s is equal to 0.4–0.7. These values are in agreement with the value of the Tafel slope found in Ref. [11] (120 mV). We compared plateau currents at various potentials as well. These currents correspond to a complex combination of processes, including the secondary nucleation and growth, 'death' of the growth of already formed particles, mass transport in solution (see, e.g., in Ref.[2]), electron transfer kinetics (see, e.g., in Ref. [1]), ohmic loss in the growing film (see, e.g., Ref. [11]). In addition, many of these processes are affected by accumulation of soluble oligomers in the vicinity of the electrode surface. Therefore, these portions of transients can be hardly analyzed in terms of any simple nucleation model. Stirring test confirms unambiguously that the growth of pTc3Py within a longer time domain takes place under the mixed control. Despite of a possible mass transport contribution, the Tafel-like dependence of the plateau current on potential is observed, i.e. a contribution of the electrochemical step is rather dominating. The Tafel slope is 0.12–0.15 V for *N*-methyl-pyrrole, in a good agreement with the α_z value mentioned above. However, the Tafel slope for plateau currents of pTc3Py deposition is significantly higher, demonstrating a more complex behavior.

Conclusions

Surely the growth of the first layer of polymer particles is only indirectly related to the morphology prediction for thicker films. However, we believe that just the films of the nm-scale thickness are of interest for fabrication of various hybrid nanomaterials (in particular metal-polymer composites), as their specific functional properties result from nm-scale phenomena.

We demonstrated that the kinetic data in terms of current transients at different potentials can be formally described in a self-consistent manner by the models of nucleation and growth proposed earlier for the metal deposition. In combination with the coulometric control it provides the instruments for control and monitoring of the thin conducting polymers deposition. Additional controllability can be achieved by formation of artificial nucleation centers, like it was done in [31] by means of HS-(CH_2)*n*-pyrrole-modification of the surface (unfortunately, the deposition was performed under less controllable potentiodynamic mode).

Our study is a primary step to understand the kinetics of polymer–metal co-deposition.

Acknowledgements This work was supported in part by the Russian Foundation for Basic Research (project No 09-03-01172a).

References

1. Asavapiryanont S, Chandler GK, Gunawardena GA, Pletcher D (1984) J Electroanal Chem 177:229–244
2. Asavapiryanont S, Chandler GK, Gunawardena GA, Pletcher D (1984) J Electroanal Chem 177:245–251
3. Kim Y-T, Collins RW, Vedom K, Allara DL (1991) J Electrochem Soc 138:3266–3275
4. Downard AJ, Pletcher D (1986) J Electroanal Chem 206:139–145
5. Downard AJ, Pletcher D (1986) J Electroanal Chem 206:147–152
6. Hamnett A, Hillman AR (1988) J Electrochem Soc 135:2517–2524
7. Soubiran P, Aeiyach S, Lacaze PC (1991) J Electroanal Chem 303:125–137
8. Bade K, Tsakova V, Schultze JW (1992) Electrochim Acta 37:2255–2261
9. Noftle RE, Pletcher D (1987) J Electroanal Chem 227:229–235
10. Hamnett A, Higgins SJ, Fisk PR, Albery WJ (1989) J Electroanal Chem 270:479–488
11. Scharifker BR, Garcia-Pastoriza E, Marino W (1991) J Electroanal Chem 300:85–98
12. Vorotyntsev MA, Casalta M, Pousson E, Roullier L, Boni G, Moise C (2001) Electrochimica Acta 46:4017–4033
13. Vorotyntsev MA, Graczyk M, Lisowska-Oleksiak A, Goux J, Moise C (2004) J Solid State Electrochem 8:818–827
14. Otero TF, Rodriguez J (1994) Electrochim Acta 39:245–253
15. Zhou M, Heinze J (1999) J Phys Chem B 103:8451–8457
16. Correia J, Graczyk M, Abrantes LM, Vorotyntsev MA (2007) Electrochim Acta 53:1195–1205
17. Vorotyntsev MA, Skompska M, Pousson E, Goux J, Moise C (2003) J Electroanal Chem 552C:307–317
18. Vassiliev SY, Denisov AV (2000) Zhurnal tehnicheskoy fiziki (in Russian) 70:100–106
19. El-Shekeil A, Al-Aghbari S (2004) Polym Int 53:777–788
20. Cosnier S, Karyakin A (eds) (2010) Electropolymerization: concepts, materials and applications. Wiley-VCH, Weinheim
21. Marcos ML, Rodriguez I, Gonzalez-Velasco J (1987) Electrochim Acta 32:1453–1459
22. Plyasova LM, Molina IYu, Gavrilov AN, Cherepanova SV, Cherstiouk OV, Rudina NA, Savinova ER, Tsirlina GA (2006) Electrochim Acta 51:4477–4488
23. Cherstiouk OV, Gavrilov AN, Plyasova LM, Molina IYu, Tsirlina GA, Savinova ER (2008) J Solid State Electrochem 12:497–509
24. Hillman AR, Mallen EF (1987) J Electroanal Chem 220:351–367
25. Rishpon J, Redondo A, Derouin C, Gottesfeld S (1990) J Electroanal Chem 294:73–85
26. Kazarinov VE, Levi MD, Skundin AM, Vorotyntsev MA (1989) J Electroanal Chem 271:193–211
27. Graczyk M (2006) Ph.D. thesis. University of Burgundy, Dijon, France
28. Randriamahazaka H, Noel V, Chevrot C (1999) J Electroanal Chem 472:103–111
29. Milchev A (2002) Electrocrystallization. Fundamentals of Nucleation and Growth. Kluwer Academic Publishers, Dordrecht
30. Milchev A (2008) J Electroanal Chem 612:42–46
31. Wurm DB, Zong K, Kim Y-H, Kim Y-T, Shin M, Jeon IC (1998) J Electrochem Soc 145:1483–1488